American Mineralogist, Volume 84, pages 15–26, 1999

Biotite dehydration, partial melting, and fluid composition: Experiments in the system $KAlO_2$-FeO-MgO-SiO_2-H_2O-CO_2

A.A. Graphchikov,[1] A.N. Konilov,[1] and J.D. Clemens[2,*]

[1]Institute of Experimental Mineralogy, Russian Academy of Science, 142432 Chernogolovka, Moscow District, Russia
[2]School of Geological Sciences, CEESR, Kingston University, Penrhyn Road, Kingston-upon-Thames, Surrey, KT1 2EE, U.K.

Abstract

Biotite solid-solutions are a significant H_2O reservoir in the lithosphere, and the assemblage Bt+Opx+Kfs+Qtz is commonly used to estimate a_{H_2O} in high-grade metamorphic and magmatic rocks. Here we report experimental constraints on subsolidus mineral equilibria involving biotite and orthopyroxene in the system $KAlO_2$-MgO-FeO-SiO_2-H_2O-CO_2. Our experiments address the question of stability of biotite of a given X_{Fe} in the assemblage Bt+Qtz±Sa, or the stability of the assemblage Opx+Sa±Qtz. Clemens (1993) and Clemens et al. (1997) concluded that CO_2 has no effect other than to lower a_{H_2O} and thereby raise the solidus T. Our data at $X^{Fl}_{H_2O} < 1$ extend these conclusions to encompass Fe-bearing systems more similar to natural rocks. From a comparison of experimental data and calculated isopleths of biotite composition in the divariant assemblage Bt+Opx+Kfs+Qtz+fluid, it appears that phlogopite-annite solid-solutions must be significantly non-ideal (at $T <$ 800 °C) or that enstatite-ferrosilite solid-solutions must have negative values for their Margules-type parameters. Ignoring these factors would result in any calculated a_{H_2O} values being too low. Although various models allow us to estimate X_{H_2O} in H_2O-CO_2 fluids, we are still unable to use biotite equilibria to estimate a_{H_2O} accurately during high-grade metamorphism and magma crystallization. We also consider qualitatively the effects Fe-Mg biotite solid-solution on partial melting equilibria in fluid-poor (rock-dominated) systems in which hydration-dehydration reactions control the fluid composition.

Introduction

Trioctahedral micas are common in magmatic and metamorphic rocks, and are significant H_2O reservoirs in the Earth's crust and upper mantle. In recent years, investigators have expended considerable energy on the determination of phase relations and crystal chemistry of these minerals. Reliable, internally consistent thermodynamic data for micas are needed for modeling dehydration and partial melting equilibria. There have been detailed studies of isomorphous substitutions in biotite involving components such as Al, Ti, and F (e.g., Circone and Navrotsky 1992; Patiño Douce 1993). Phlogopite [$KMg_3AlSi_3O_{10}(OH)_2$]-annite [$KFe_3AlSi_3O_{10}(OH)_2$] solid-solutions are commonly treated as ideal, an assumption based mainly on the distribution of Fe and Mg between biotite and other ferromagnesian silicates (e.g., Mueller 1972). The present work focuses on equilibria in the system $KAlO_2$-MgO-FeO-SiO_2-H_2O-CO_2, as models for dehydration and partial melting reactions involving biotite (e.g., Grant 1985). The following phases may participate in these equilibria: quartz (Qtz); biotite (Bt), phlogopite-annite (Phl-Ann); high sanidine (Sa); orthopyroxene (Opx), enstatite-ferrosilite (En-Fs); silicate melt (M); and supercritical fluid (Fl), H_2O-CO_2.

Our new data allow us to examine further the validity of the hypothesis of a special role for CO_2 in partial melting reactions involving Fe-Mg biotites (e.g., Hansen et al. 1984; Grant 1985; Peterson and Newton 1989b, 1990). This hypothesis is founded upon the experimental data of Wendlandt (1981) and Peterson and Newton (1990). According to these authors, melting of the assemblage Phl+Sa+Qtz in the presence of an H_2O-CO_2 fluid with $X_{H_2O} = 0.5$ (where X_{H_2O} is the mole fraction of H_2O in the fluid phase) may take place at a T lower than melting in the presence of a pure H_2O fluid. These unexpected results were not confirmed in the experiments of Clemens (1993) and Clemens et al. (1997), who refuted the conclusions of Peterson and Newton (1989b, 1990). Our present study examines whether the addition of Fe to the system has any effect on the role of CO_2.

Experimental details

Starting materials

The starting charges consisted of mixtures of synthetic minerals. The compositions of the charges are given in Table 1. Biotites of the phlogopite-annite series, with X_{Fe} [Fe/(Fe + Mg)] = 0.3 and 0.5, and high sanidine were synthesized hydrothermally from gels. Biotites with other compositions and orthopyroxenes were synthesized from K_2CO_3, $Al(OH)_3$, $MgC_2O_4 \cdot 2H_2O$, $FeC_2O_4 \cdot 2H_2O$, and X-

* E-mail: J.Clemens@kingston.ac.uk

0003–004X/99/0102–0015$05.00

TABLE 1. Experimental results in the system $KAlO_2$-MgO-FeO-SiO_2-H_2O-CO_2

Experiment no.	T (°C)	P (MPa)	Duration (days)	Starting material mass (mg) Bt	Qtz	Sa	Opx	X_{Fe} Bt or Opx	Run products*	Final X_{H_2O}
				Initial X_{H_2O} = 0.5						
1804	650	400	10	10	10	tr.	–	0.74 ± 0.03	Bt+**Qtz**+**Sa**+**Opx**	NA
1799	700	400	10	10	10	–	–	0.53 ± 0.03	Bt+**Qtz**+**Sa**+**Opx**	NA
1800	700	450	10	20	5	–	–	0.54 ± 0.03	**Bt**+Qtz+**Sa**+**Opx**	NA
1610	700	500	7	10	7	3	–	0.68 ± 0.04	Bt+**Qtz**+**Sa**+**Opx**	0.546
1674	700	500	6	11	7	3	–	0.70 ± 0.02	Bt+**Qtz**+**Sa**+**Opx**	NA
1809	700	500	10	–	+	+	+	0.50 ± 0.03	**Bt**+**Qtz**+**Sa**+Opx	0.532
1801†	750	400	10	20	5	–	–	0.30 ± 0.02	**Bt**+Qtz+**Sa**+**Opx**	NA
1805†	750	400	10	–	–	1.5	4.5	0.25 ± 0.03	**Bt**+**Qtz**+**Opx**+Sa	0.510
1661	750	500	6	10	7	8	–	0.48 ± 0.02	Bt+**Qtz**+**Sa**+**Opx** (tr.)	0.504
1662	750	500	6	10	10	–	–	0.44 ± 0.03	Bt+**Qtz**+**Sa**+**Opx**	0.502
1810	750	500	5	–	+	+	+	0.30 ± 0.03	Bt+**Qtz**+**Sa**+**Opx**	NA
1794	770	1000	4	4.5	4.5	–	–	0.50 ± 0.02	**Bt**+**Qtz**	NA
1693	800	450	5	10	10	–	–	0.53 ± 0.04	Bt(tr.)+**Qtz**+**Sa**+**Opx**	0.538
1777‡	800	500	5	+	+	–	+	0.84/0.83 ±0.02/±0.02	**Qtz**+**Sa**+**Opx**	0.513
1795†	850	1000	4	4.3	4.3	–	–	0.29 ± 0.03	Bt+**Qtz**+**Opx**+**M**	NA
				Initial X_{H_2O} = "0.0"						
1566	730	500	7	20	3	–	–	0.47 ± 0.07	**Bt**+**Sa**+**Opx**	0.099
1543	750	500	7	10	20	–	–	0.47 ± 0.07	Bt(tr.)+**Qtz**+**Sa**+**Opx**	0.116
1520	750	500	7	6	14	20	–	0.30 ± 0.02	**Qtz**+**Sa**+**Opx**	0.045
1608	750	500	7	10	27	3	–	0.48 ± 0.02	**Qtz**+**Sa**+**Opx**	0.125
1578	800	400	7	10	10	15	–	0.47 ± 0.07	**Qtz**+**Sa**+**Opx**	0.118

Notes: X_{Fe} = Fe/(Fe + Mg), X_{H_2O} = H_2O/(H_2O + CO_2), ± values = mean-square deviation, + = phase present, – = phase absent, tr. = trace, NA = not analyzed, minerals in run products listed in the order of decreasing abundance.

* Assumed equilibrium phases in bold.

† In run products: 1801 – X_{Fe}^{Opx} = 0.43 ± 0.02, 1805 – X_{Fe}^{Bt} = 0.22 ± 0.03, 1795 – X_{Fe}^{Opx} = 0.27 ± 0.02.

‡ Run 1777 starting material contained glass (quenched melt).

ray-amorphous SiO_2. Synthesis conditions were 700 °C, 300 MPa, and 7 d. For synthesis of biotite and sanidine, 50 mg of oxalic acid dihydrate were added for each 100 mg of gel mixture, with no additional fluid. Pure quartz was obtained by crushing a synthetic monocrystal.

Synthetic biotite formed pseudohexagonal scaly crystals or rounded grains up to 10 μm across. Generally, no other phases were present. However, in some cases a few crystals of sanidine formed. Synthetic orthopyroxene formed prisms up to 40 μm long. X-ray diffraction (XRD) methods (Wones 1963; Fonarev and Konilov 1986) and electron microprobe analyses were used to determine the biotite and orthopyroxene starting compositions. Values of X_{Fe} in biotites synthesized from gels were determined from the 2θ values of 060 and $\bar{3}31$ X-ray reflections. This method produced results identical to the microprobe analyses. The variance (σ^2) in X_{Fe} for these biotites was <0.02. Biotite and orthopyroxene crystals synthesized from mixtures of chemical reagents were rather more heterogeneous (σ^2 of X_{Fe} = 0.02 to 0.07).

Apparatus

Experiments at pressures up to 500 MPa were carried out in externally heated cold-seal vessels pressurized with H_2O, in the Institute of Experimental Mineralogy, Chernogolovka. The split furnaces have hot spots with gradients of 2–3 °C over 50 mm where the capsules were placed. Temperatures were measured with chromel-alumel (type-K) thermocouples, with overall accuracies of ±5 °C. Attainment of desired experimental conditions required 1.5 to 2 h. Each experiment was quenched by a blast of cold compressed air. Over the 10–12 min of quenching, the temperature decreased to between 150 and 200 °C. Pressures were measured by tube manometers with accuracies of ±10 MPa.

All these experiments were carried out with starting materials in welded gold capsules, with wall thicknesses of 0.1 or 0.2 mm. Given that the vessels generate an intrinsic hydrogen fugacity close to Ni-NiO-H_2O (NNO), we abandoned the use of double capsules. Instead we used additional nickel capsules (30 mm long) filled with NNO buffer mixture, placed near the sample capsules in the vessels. In experiments with $X_{H_2O} < 1$, the f_{O_2} was lower than NNO, since f_{O_2} is proportional to $f_{H_2O}^2$, and therefore approximately to $X_{H_2O}^2$. Thus, for X_{H_2O} = 0.5, log f_{O_2} was about 0.6 units below NNO, and for X_{H_2O} = 0.1, log f_{O_2} was 2.0 units below NNO.

At higher pressures, experiments were carried out in a non-end-loaded piston-cylinder apparatus at Manchester University, using NaCl-MgO cells and with *T* measured by Pt-$Pt_{87}Rh_{13}$ (type-R) thermocouples. Detailed descriptions of the apparatus and pressure cells are given in Vielzeuf and Clemens (1992) and Clemens (1995). Previous calibrations with this type of cell suggest that f_{O_2} was very close to NNO for experiments with X_{H_2O} = 1.

METHODS

The composition of the starting mixture was either on the Bt-Qtz or Sa-Opx compositional join, or in the Bt-Sa-Qtz, Qtz-Sa-Opx, or Bt-Qtz-Opx field (see Fig. 1).

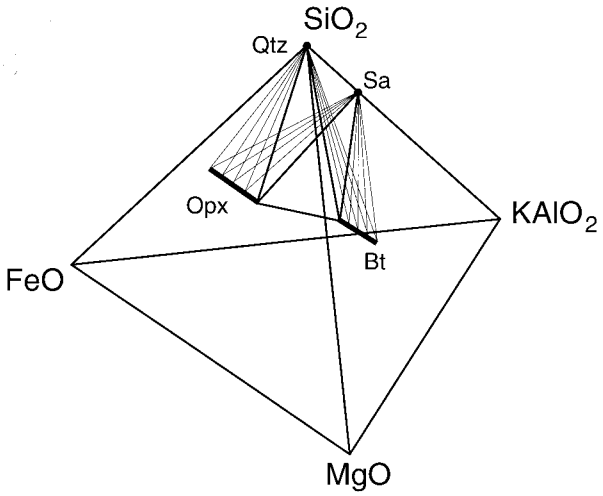

FIGURE 1. $KAlO_2$-MgO-FeO-SiO_2 tetrahedron illustrating phase compatibility relations among biotite, orthopyroxene, sanidine, and quartz in the fluid-saturated system $KAlO_2$-MgO-FeO-SiO_2-H_2O-CO_2, at fixed P, T, and X_{H_2O}. The divariant, four-phase assemblage is shown with its bounding three-phase assemblages (with thin lines showing the compositional variation in biotite and orthopyroxene). Qtz+Opx+Bt is the limiting assemblage discussed with reference to Figures 2 and 3. See text for further discussion.

Starting mixtures (15–30 mg) were ground under acetone in an agate mortar for 15–30 min. The mixtures were then air dried and loaded into the capsules. Initial X_{H_2O} was controlled by adding 30 mg of oxalic acid dihydrate $H_2C_2O_4 \cdot 2H_2O$ (for $X_{H_2O} = 0.5$) or 50 mg of silver oxalate $Ag_2C_2O_4$ (for $X_{H_2O} \approx 0$) to the capsules. The capsules were then dried at 110 °C for 30 min and promptly welded shut. Durations of experiments in cold-seal vessels were limited by the period over which buffer mixtures would allow control of f_{O_2}. They varied between 4 and 10 d, depending on the P and T of the experiment. Piston-cylinder experiments were of 4 d duration.

Examination and interpretation of experimental products

Products of the experiments were studied in optical grain mounts and by XRD methods. Values for final X_{H_2O} were determined by measuring sequential capsule mass losses on puncture (mass of CO_2) and heating at 120 °C (mass of H_2O). This method is considered valid because, at the conditions of the experiments, the total mole fraction of fluid species other than H_2O and CO_2 should be <0.006 (according to calculations carried out using the program COHSgraph 3.3; Holloway 1987). For experiments with initial $X_{H_2O} = 0.5$, final X_{H_2O} was not always determined, because all previous measurements had yielded consistent results with final X_{H_2O} between 0.50 and 0.55. For experiments with initial X_{H_2O} supposedly at 0, final X_{H_2O} was always determined, and differed markedly from the theoretical value in every case. Apart from the presence of adsorbed H_2O in $Ag_2C_2O_4$, H_2O is evolved during subsolidus biotite breakdown. Thus, it is impossible to obtain a pure CO_2 fluid in such experiments.

RESULTS

Figure 1 illustrates the possible equilibrium phase fields in the fluid-saturated tetrahedron $KAlO_2$-MgO-FeO-SiO_2, at fixed P, T, and X_{H_2O}. The divariant four-phase volume Bt-Opx-Sa-Qtz is shown with the bounding three-phase assemblages Bt+Sa+Qtz, Bt+Opx+Qtz, Bt+Opx+Sa, and Opx+Sa+Qtz. Except in extremely Fe-rich systems, Bt+Sa+Qtz will be stable at low X_{Fe} and Opx+Sa+Qtz at high X_{Fe}. In accordance with the results of previous experimental and field studies of coexisting Bt and Opx, we show the mica as containing slightly more magnesium than coexisting orthopyroxene (e.g., Fonarev and Konilov 1986). Again, except in extremely Fe-rich systems the models of Fonarev and Konilov (1986) show that K_D ($= X_{Fe}^{Bt}/X_{Fe}^{Opx}$) increases at higher T.

Most products of experiments at $T < 770$ °C, $P = 400$–500 MPa, and initial $X_{H_2O} = 0.5$ contain four-mineral assemblages (Table 1). However, since complete equilibrium is not achieved at these conditions, such results represent disequilibrium, rather than divariant assemblages. The sluggish kinetics of such reactions have been noted previously (e.g., Vielzeuf and Clemens 1992; Clemens 1995) and are responsible for the metastable persistence of Bt in 1610 and Opx in 1809, for example. In Table 1, mineral phases belonging to the assumed stable assemblages are printed in bold type (see also Fig. 1).

Products of experiments at $T > 770$ °C or at initial $X_{H_2O} \approx 0$ are three-mineral assemblages. The only exceptions are 1566, 1693, and 1543, which contain traces of the starting biotite. In these higher-temperature experiments, the sluggish kinetics are overcome; one of the starting phases disappears completely and a new phase is formed, which suggests a closer approach to equilibrium. It is interesting that, in experiments with initial $X_{H_2O} \approx 0$, a high degree of reaction is observed, even for T as low as 750 °C.

With a starting assemblage of Sa+Opx±Qtz±Bt (experiments 1809, 1805, and 1810) the composition of newly formed biotite was determined only in the products of experiment 1805 (Table 1). In the other cases, the very small grain-size of the biotite made it impossible to obtain quantitative electron probe analyses. In experiment 1794 (770 °C and 1000 MPa) the biotite+quartz starting assemblage remained stable. Because new phases always formed, even at lower T, it follows that this represents the equilibrium assemblage. Thus, we cannot claim to have produced a divariant assemblage in any of our experiments. We have only addressed the question of the stability of biotite with a given X_{Fe} in the assemblage Bt+Qtz±Sa, or the stability of the assemblage Opx+Sa±Qtz. In Figure 2, the results are shown in terms of whether the divariant assemblage would contain biotite with X_{Fe} greater or less than that in the starting material, at the particular P-T conditions of the experiment.

Glass (quenched melt) occurred only in the product of

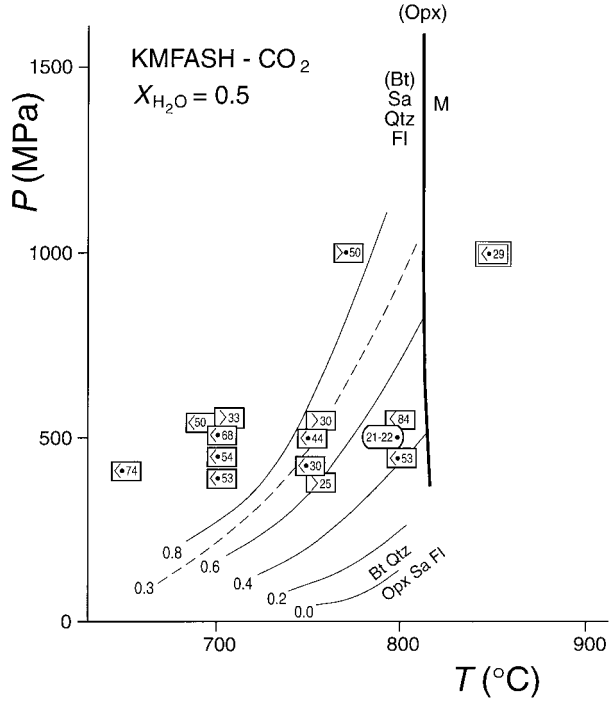

FIGURE 2. Experimental data and calculated isopleths of biotite composition in mole fractions of the annite component (X_{Ann}) in the divariant assemblage Bt+Opx+Sa+Qtz+Fl at X_{H_2O} = 0.5, assuming ideal mixing between Ann and Phl end-members. Values in rectangles (present work) and ovals (Konilov and Fonarev 1993) correspond to $100X_{Ann}$ (mol% annite, ± 2 mol%) values from experimental data. The symbol < indicates that the *P-T* conditions of the experiment correspond to an isopleth with $100X_{Ann}$ lower than the value shown; the > symbol indicates the opposite relationship. Where two values of $100X_{Ann}$ are shown in a rectangle or oval these represent the range of biotite compositions found in the experiment. The double rectangle represents experiment 1795 (Table 1) in which melting occurred. The small dots indicate the actual experimental points. In cases without dots, the experimental points are coincident with those in adjoining rectangles or ovals. Redundant experiments 1661 and 1674 (Table 1) are not plotted. The locus of Sa+Qtz+Fl = M (Bohlen et al. 1983) is shown as a model for Bt+Sa+Qtz+Fl = M (see text). The dashed line represents the position of the X_{Ann} = 0.3 isopleth as inferred from the experiments. Note that this does not correspond to the calculated position for the assumption of ideal Fe-Mg mixing in the biotite (see text).

experiment 1795 (850 °C, 1000 MPa, and initial X_{H_2O} = 0.5). These conditions exceed those required for sanidine-quartz melting under the same conditions (Fig. 2). In experiment 1777, at conditions outside the melting range of sanidine-quartz, at X_{H_2O} = 0.5, the starting glass was consumed and only the crystalline subsolidus assemblage was present. The products of all experiments made at initial $X_{H_2O} \approx 0$ (and final $X_{H_2O} \approx 0.1$) contain subsolidus assemblages. These data are entirely compatible with the inference, drawn by Clemens (1993) and Clemens et al. (1997), regarding the role of carbon dioxide in metamorphism and melting, that CO_2 has no effect other than to lower a_{H_2O} and thereby to raise the solidus *T*.

Theoretical considerations

In the system under investigation, the partitioning of Fe and Mg between biotite and orthopyroxene can be described by the exchange equilibrium:

$$KFe_3AlSi_3O_{10}(OH)_2 + 3MgSiO_3 = KMg_3AlSi_3O_{10}(OH)_2 + 3FeSiO_3 \quad (1)$$

and subsolidus equilibria in orthopyroxene-bearing quartzofeldspathic rocks can be modeled by the reaction:

$$KMg_3AlSi_3O_{10}(OH)_2 + 3SiO_2 = KAlSi_3O_8 + 3MgSiO_3 + H_2O. \quad (2)$$

For Equilibrium 1, we can write:

$$\Delta G_1 + 3RT \ln a_{Fs} + RT \ln a_{Phl} - 3RT \ln a_{En} - RT \ln a_{Ann} = 0 \quad (3)$$

and for equilibrium 2:

$$\Delta G_2 + RT \ln f_{H_2O} + 3RT \ln a_{En} - RT \ln a_{Phl} = 0 \quad (4)$$

with:

$$f_{H_2O} = P_{H_2O} \cdot \Gamma_{H_2O} \cdot X_{H_2O} \cdot \gamma_{H_2O} \quad (5)$$

and

$$X_{H_2O} = n_{H_2O}/(n_{H_2O} + n_{CO_2}) \quad (6)$$

in which Γ_{H_2O} is the fugacity coefficient of pure H_2O, γ_{H_2O} is the activity coefficient for H_2O in the H_2O-CO_2 mixture, X_{H_2O} is the mole fraction of H_2O in the fluid phase, and n is the number of moles of the subscripted species in the fluid. We used the modified Redlich-Kwong equation of state for H_2O-CO_2 mixtures given by Kerrick and Jacobs (1981).

Figures 2 and 3 show calculated compositional isopleths for biotite in equilibrium with orthopyroxene, sanidine, quartz, and fluid at X_{H_2O} = 0.5 and 1.0, based on the thermodynamic data listed in Table 2 and assuming ideal mixing in the Phl-Ann system. At high temperatures, isopleths are truncated by the univariant reaction: Bt+Sa+Qtz+Fl = M. Due to the small amounts of FeO and MgO soluble in the melts at moderate temperatures, the position of this reaction must be very close to that of the univariant reactions Phl+Sa+Qtz+Fl = M and Sa+Qtz+Fl = M (Vielzeuf and Clemens 1992; Clemens 1995). Calculated isopleths shift considerably to lower temperatures with decreasing X_{H_2O} and increasing X_{Fe} in biotite. However, there is a major discrepancy between the calculated and experimentally constrained shifts (see later discussion).

Figure 4 shows the calculated locus of the Fe-free univariant equilibrium Phl+Qtz = En+Sa+H_2O (reaction 2) as a function of X_{H_2O} in an H_2O-CO_2 fluid. Thermodynamic data (except for the mixing parameters for solid-solutions) were taken from Holland and Powell (1990). Calculations using these data do not satisfactorily reproduce

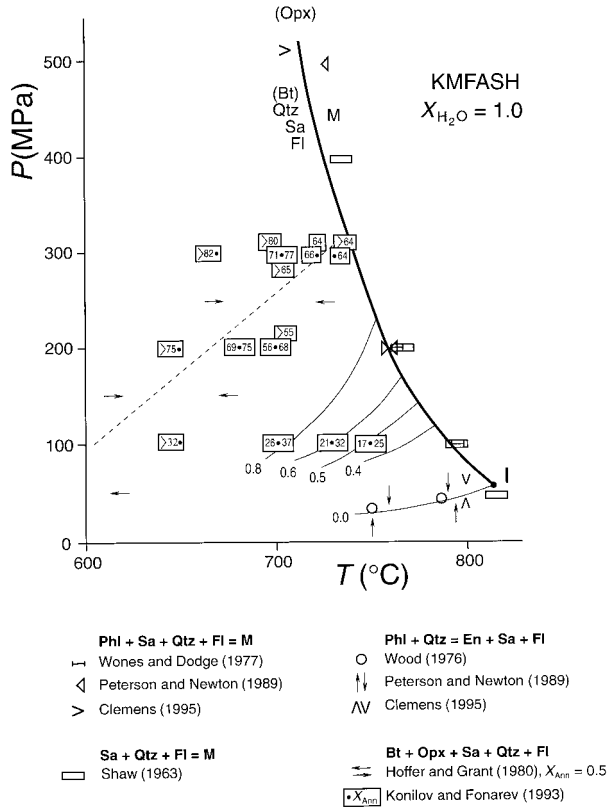

FIGURE 3. Experimental data and calculated isopleths (thin lines) of biotite composition (X_{Ann}) in the divariant assemblage Bt+Opx+Sa+Qtz+Fl at X_{H_2O} = 1. The thick dashed line is the approximate position of this same reaction (for X_{Ann} = 0.5) based on the experiments of Hoffer and Grant (1980). The evident discrepancy between calculated and experimentally located isopleths is discussed in the text. Numbers in rectangles correspond to $100X_{Ann}$ for experimental data (Konilov and Fonarev 1993). The > symbols have the same meaning as in Figure 2. In rectangles without dots, the experimental points are coincident with those in adjoining rectangles. The position of the reaction Bt+Sa+Qtz+Fl = M is shown consistent with the results of Shaw (1963), Wones and Dodge (1977), Peterson and Newton (1989a), Vielzeuf and Clemens (1992), and Clemens (1995). The point labeled I is the invariant point in the Fe-free system.

the experimental data for Equilibrium 2 at X_{H_2O} = 1 (Figs. 3 and 4). This is apparent in Figure 3, where the calculated isopleth for X_{Ann} in biotite = 0.5 is at a T up to 150 °C higher than the location inferred from the experiments of Hoffer and Grant (1980). For X_{H_2O} = 0.5, Figure 2 shows the position of the X_{Ann} = 0.3 isopleth inferred from the experiments (dashed line), which can be compared to the calculated position. Again, the discrepancy is large and apparent.

One source of uncertainty here may be in the value of S^0_{Phl}, due to the possibility of order-disorder on tetrahedral Si-Al sites (e.g., Clemens et al. 1987). The value for S^0_{Phl} probably lies between 315.9 and 335 J/mol·K (Circone and Navrotsky 1992). Vinograd (1995) estimated the Al-Si configurational entropy of phlogopite as 11 ± 1 J/mol·K, which yields S^0_{Phl} = 326.9 ± 1 J/mol·K, very close to the value of 325 J/mol·K given by Holland and Powell (1990). Another parameter that might be incorrect is the standard enthalpy of formation of phlogopite. Replacement of the value $\Delta H^0_f = -6211760$ J/mol (Holland and Powell 1990) by −6216780 J/mol would allow the experimental data (for Equilibrium 2 at X_{H_2O} = 1) to be reproduced. This ΔH^0_f value is within the error limits imposed by the high-temperature solution calorimetry (Clemens et al. 1987; Circone and Navrotsky 1992) and was derived by assuming that all other thermodynamic parameters for phases involved are correct and by simply adjusting ΔH^0_f until the position of the calculated equilibrium agreed with the experimental constraints.

Equilibrium 2 has been studied by many previous researchers (e.g., Wood 1976; Wones and Dodge 1977; Clemens 1995) and the *P-T* locus calculated with the adjusted ΔH^0_f value for phlogopite agrees well with these studies. The most recent work, by Berman et al. (1995), appears to be discrepant with these previous studies. Aranovich and Newton (1998) prefer the Berman et al. location for the reaction, and suggest that the lack of filler rods and the consequent occurrence of thermal convection may have caused errors of T measurement with external thermocouples in the previous experiments using cold-seal vessels. This explanation is most unlikely because the vessels (at Clermont-Ferrand) used by Clemens (1995) are vertically mounted and ceramic filler rods are always employed (Vielzeuf and Clemens 1992). As mentioned in Clemens (1995), the internal-external thermal gradients were carefully measured for these vessels and found to be negligible (<1 °C). We therefore prefer the earlier experimental results. In the system KMFASH-CO_2, Equilibrium 2 occurs at P < 100 MPa. Below, in the section on the silicate component of the fluid phase, we discuss the influence of pressure on mineral solubility and the position of this equilibrium in KMFASH-CO_2.

A comment on mixing parameters

Due to the experimental uncertainties, we are unable to use our data to extract reliable interaction parameters for biotite solid-solutions. However, we can make some qualitative comments and it seems worthwhile to discuss briefly the problem of mixing parameters.

The end-members of orthopyroxene solid-solutions are taken as $MgSiO_3$ (enstatite) and $FeSiO_3$ (ferrosilite). There are contradictory literature values for the Margules-type terms used to describe the non-ideal mixing of enstatite and ferrosilite components ($W_{En\text{-}Fs}$). Hayob et al. (1993) made a complete analysis of the available data on En-Fs solid-solution and showed that $W_{En\text{-}Fs}$ must have a small positive value of 3600 ± 4900 J/mol, with W_V = 0 and W_S = 0. In a recent thermodynamic study, Carpenter and Salje (1994) also obtained a positive value for the excess energy of mixing along the enstatite-ferrosilite join.

In our system, biotites can be satisfactorily described

TABLE 2. Molar thermodynamic data

Phase	End-member	Composition
α-quartz (α-Qtz)		SiO_2
β-quartz (β-Qtz)		SiO_2
High sanidine (Sa)		$KAlSi_3O_8$
H_2O fliud		H_2O
Biotite (Bt)	Phlogopite (Phl)	$KMg_3AlSi_3O_{10}(OH)_2$
	Annite (Ann)	$KFe_3AlSi_3O_{10}(OH)_2$
Orthopyroxene (Opx)	Enstatite (En)	$MgSiO_3$
	Ferrosilite (Fs)	$FeSiO_3$

Phase/Component	ΔH_f^0 (kJ)	S^0 (J/K)	a	b × 10^2	c × 10^{-3}	d × 10^{-3}	V^0 (J/bar)
α-Qtz	−910.800	41.50	97.9	−0.3350	−636.20	−0.7740	2.269
β-Qtz	−914.397	30.16	57.9	0.9330	1834.71	0.0000	2.372
Sa	−3959.060	230.00	448.8	−1.0075	−1007.30	−3.9731	10.892
H_2O	−241.810	188.80	40.1	0.8656	487.50	−0.2512	
Phl	−6216.780	326.90	770.3	−3.6939	−2328.90	−6.5316	14.964
Ann	−5149.320	414.00	815.7	−3.4861	19.80	−7.4667	15.432
En	−1544.690	66.25	178.1	−0.1495	−298.45	−1.5927	3.131
Fs	−1194.095	94.70	178.7	−0.1378	−355.55	−1.4963	3.296

Notes: With exceptions given below, all data from Holland and Powell (1990), including mineral compressibilities and thermal expansivities not given in the table; $C_p = a + bT + c/T^2 + d/T^{0.5}$. Exceptions: most data for β-Qtz from Hemingway (1987) and thermal expansion coefficient from Nicholls and Stout (1982); MRK equation of state for H_2O-CO_2 mixtures from Kerrick and Jacobs (1981); $\Delta H^0_{f\,Phl}$, S^0_{Phl}, and S^0_{Fs} from this work. $\Delta H^0_{f\,Phl}$ value is subject to error introduced by dissolution of silicates into the fluid phase, affecting a_{H_2O}.

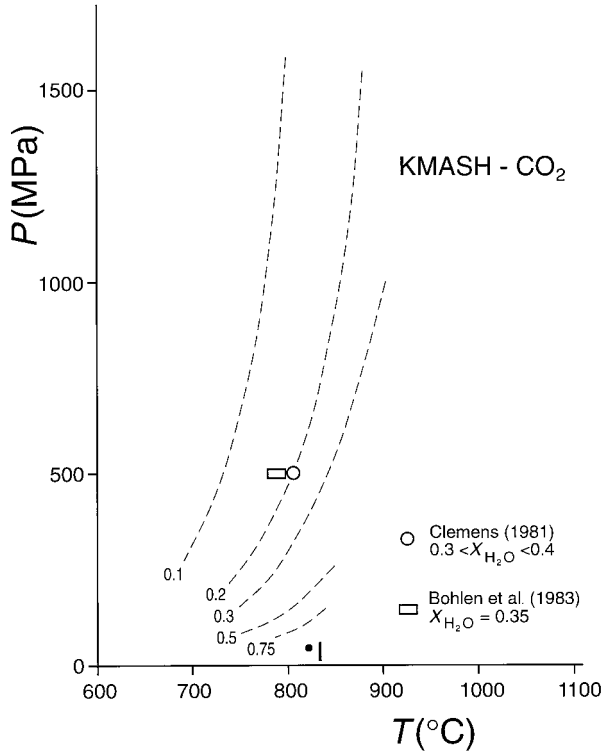

FIGURE 4. Experimental data and calculated position (dashed lines) of the univariant dehydration reaction Phl + 3Qtz = 3En + Sa + H_2O (Equil. 2) at various X_{H_2O} values. Experimental reversals, in T-X_{H_2O} space (Clemens 1981; Clemens et al. 1997) and P-T space (Bohlen et al. 1983) are shown for comparison. The dot labeled I is the invariant point in the KMASH system (Clemens 1995). See Figure 5 for the complete phase relations in this system.

as solid-solutions of phlogopite [$KMg_3AlSi_3O_{10}(OH)_2$] and annite [$KFe_3AlSi_3O_{10}(OH)_2$]. According to the data of Patiño Douce et al. (1993), for ideal biotite solid-solutions in this series:

$$a_{Phl} = \frac{256}{27}(X_{Mg})^3 \cdot X_{Al}(X_{Si})^3 \cdot X_K(X_{OH})^2. \quad (7)$$

In all calculations we assumed that all iron is Fe^{2+}. Strictly speaking, this cannot be correct but the relatively low f_{O_2} values in the experiments would have resulted in low Fe^{3+} concentrations. In our experiments, the biotites were always K deficient, with apparent X-site occupancies (0.85–0.95) similar to those in natural biotites. It also seems likely that there will be analytical errors in the measured K concentrations (e.g., Van der Pluijm et al. 1988). Thus, we took the expedient of setting $X_K = 1$. Lack of data for X_{OH}, and the fact that F and Cl components were not present, lead us to use $X_{OH} = 1$. Taking $X_{Si} = Si/4 = 0.75$ and $X_{Al} = Al/4 = 0.25$, we obtain, for an ideal solid-solution:

$$a_{Phl} = X^3_{Mg} \quad (8)$$

For non-ideal Fe-Mg mixing:

$$a_{Phl} = (X_{Phl} \cdot \gamma_{Phl})^3 \quad (9)$$

and

$$RT \ln \gamma_{Phl} = X^2_{Ann}[W_{Phl\text{-}Ann} + 2X_{Phl}(W_{Ann\text{-}Phl} - W_{Phl\text{-}Ann})] \quad (10)$$

with

$$X_{Phl} = Mg/(Fe + Mg) \quad (11)$$

and

$$X_{Ann} = Fe/(Fe + Mg) \quad (12)$$

Similarly, for the annite end-member:

TABLE 3. Composition (normalized to 100 wt% anhydrous) of quenched fluid in the system $KAlO_2$-MgO-FeO-SiO_2-H_2O-CO_2 at P = 500 MPa.

Experiment no.	1659	554	201	392
T (°C)	650	700	750	800
Duration (days)	10	8	14	6
Assemblage	(Bt + Sa + Qtz)	(Bt + Opx + Qtz)	(Bt + Opx + M)	(Bt + Opx + M)
SiO_2	90.34 (1.26)	85.17 (2.51)	86.73 (2.49)	87.95 (2.76)
Al_2O_3	4.84 (0.06)	7.67 (1.62)	6.15 (1.50)	5.18 (1.33)
FeO	—	0.57 (0.32)	1.87 (1.28)	1.55 (0.57)
MgO	—	0.04 (0.09)	0.43 (0.46)	0.01 (0.02)
K_2O	4.82 (1.32)	6.55 (0.91)	4.82 (0.88)	5.31 (1.23)
Al/K	0.97 (0.27)	1.07 (0.15)	1.18 (0.24)	0.87 (0.05)
n	2	18	10	9
counting time (s)	10	10	10	70

Note: Values in parentheses = mean-square deviations; n = number of individual analyses. For description of the runs see Graphchikov and Konilov (1996).

$$a_{Ann} = (X_{Ann} \cdot \gamma_{Ann})^3 \quad (13)$$

and

$$RT \ln \gamma_{Ann} = X_{Phl}^2[W_{Ann\text{-}Phl} + 2X_{Ann}(W_{Phl\text{-}Ann} - W_{Ann\text{-}Phl})] \quad (14)$$

Given the absence of excess volumes of mixing along the phlogopite-annite join (Wones 1963), the value of W_V can reasonably be taken as 0.

In contrast to orthopyroxene solid-solutions, Phl-Ann mixing is commonly modeled as ideal. The basis of this assumption is the Fe-Mg distribution in natural biotites (e.g., Mueller 1972) and experimental data on element partitioning between coexisting biotite and garnet (Ferry and Spear 1978; Perchuk and Lavrent'eva 1983). Relatively few authors treat Phl-Ann mixing as non-ideal (e.g., Sack and Ghiorso 1989; Bhattacharya et al. 1992). Calculation of mineral equilibria with any of the published models for Opx solid-solution shows that the assumption of ideal Phl-Ann mixing does not allow us to reproduce the experimental data satisfactorily.

As noted above, there are serious discrepancies between experimentally located isopleths and those calculated by treating both biotite and orthopyroxene as ideal solid-solutions (see Figs. 2 and 3). Since the experimentally produced biotites have lower X_{Ann} than expected for ideal mixing, we can infer positive values of $W_{En\text{-}Fs}$. It is probable that cation ordering results in significant negative deviations from ideality in orthopyroxene solid-solutions (Aranovich and Kosyakova 1986; Carpenter and Salje 1994). A negative value of W (e.g., Aranovich and Podlesskii 1989) would not permit satisfactory reproduction of the experimental data. The consensus seems to be that small degrees of nonideality are likely in biotite solid-solutions.

Analyses of biotite compositions in experimental products shows that biotite in assemblages with Opx and Sa undergoes changes in X_{Fe}, generally incorporates some "excess" Al, and is deficient in K. According to Equation 7 use of $X_K < 1$ reduces a_{Phl}. This results in much larger values for $W_{Phl\text{-}Ann}$ and $W_{Ann\text{-}Phl}$. The number of Al cations (based on 11 O atoms per formula unit) is about 1.1 (e.g., Graphchikov and Konilov 1996, Table A2). "Excess" Al can replace Fe, Mg, and Si in Tschermak-type substitutions. If "excess Al" replaces Si, then X_{Al} is about 0.275 (instead of 0.25) and X_{Si} will be lowered simultaneously to 0.725. According to Equation 7 the overall effect will be a small reduction in a_{Phl}, but it is also necessary to take into account non-ideal Al-Fe and Al-Mg interactions (see Circone and Navrotsky 1992; Patiño Douce et al. 1993).

Silicate solubility in the fluid phase

An additional source of uncertainty in any thermodynamic calculations arises from the assumption that the experimental fluid phases are either pure H_2O or H_2O-CO_2. Products of experiments performed in KMFASH at $P > 200$ MPa (this work; Graphchikov and Konilov 1996) contain optically isotropic particles with a refractive index <1.48. In the products of experiments at $P <$ 200 MPa, there are no such isotropic particles. This material appears to be a silicate gel precipitated from the fluid phase during the quench. It usually forms spheroids, though ribbon-like masses are also present, overgrowing or adhering to crystals. The presence of similar gel-like material has been noted by many investigators (e.g., Shaw 1963; Yoder and Kushiro 1969; Wendlandt and Eggler 1980; Peterson and Newton 1989a; Clemens 1995). Such gels could be the equivalents of what Wilkinson et al. (1996) described as "silicothermal" fluids, which are relatively low-T, highly siliceous substances identified in fluid inclusions, and which are apparently immiscible with coexisting aqueous fluids.

Compositions of these gel particles were determined by electron microprobe analysis and are given in the Table 3. The concentrations of FeO and MgO are very low and values of Al/K are close to those in the starting mixture (i.e., ≈1). Thus, the gels seem to be neither peralkaline nor peraluminous. In our experimental products, the equilibria can be described in the six-component system K_2O-Al_2O_3-MgO-FeO-SiO_2-H_2O. However, the low degrees of Tschermak substitution in Bt and Opx suggest that the divariance introduced by this factor is unlikely to be significant (see above). To form these silica-rich gels,

excess quartz needs to be present in the starting material, but gel composition is independent of the precise amount of excess quartz. From the occurrence of electron beam damage in the gel spheres, we conclude that H_2O is also a significant component of the particles.

In experiments with H_2O-CO_2 fluids, gel formation is strongly inhibited at lower X_{H_2O}. However, gel is present even in the products of the experiments performed at X_{H_2O} = 0.1–0.2. Unfortunately, the very small quantity and size of the gel particles in these particular experimental products prevented determination of their composition.

The quantity of dissolved silicate component in the fluid can be estimated from experiments with various quantities of quartz in the starting mixtures. Some experimental products contain no quartz. Knowing the initial quantity of quartz and the composition of the gel particles, we can estimate the quantity of dissolved silicate. With T = 750 °C, P = 500 MPa, X_{H_2O} = 1, and a fluid to solid mass ratio of 1:1, we estimate that about 7 wt% of the original solid charge was dissolved in the fluid phase. The degree of dissolution increases with temperature, pressure, and increasing Fe content of the charge. In experiments at 500 MPa, gel formation still occurs at T as low as 650 °C. Our data agree with the conclusion of Wendlandt and Eggler (1980) that formation of detectable quantities of gel requires a fluid to solid ratio of least 0.1 to 0.15.

From these data we infer that, with the increasing T, P, X_{H_2O}, and X_{Fe} in the system KMFASH-CO_2, the silicate content of the fluid phase will increase. A decrease in X_{H_2O} (and a_{H_2O}), and some shift in the positions of equilibria and mineral composition isopleths toward lower T are inevitable consequences of this. However, it is presently impossible to apply a suitable correction factor to the activities of fluid components.

Discussion and geological applications

Estimation of H_2O activity

The assemblage Bt+Opx+Kfs+Qtz is commonly used to estimate a_{H_2O} in granulite-facies metamorphic rocks. In such calculations, biotite solid-solution has always been taken as ideal. Clemens (1995) noted that lack of knowledge of the mixing properties of phases involved probably represents the greatest single impediment to the use of the calculated equilibria. Experimental data indicate that the P-T positions of biotite dehydration reactions strongly depend on X_{Fe} of the participating minerals. However, using current models for biotite and orthopyroxene solid-solutions, we cannot even approximately model mineral equilibria in the system KMFASH-CO_2. Figure 3 shows that the assumption of ideality will result in the calculated position of reaction 2 being at too high a temperature for any given biotite composition. Thus, for a given rock P and T (from geothermometry and geobarometry) this kind of calculation would result in a considerable underestimation of a_{H_2O}, although we cannot be precise about the magnitude of this error.

For fluid-present systems, with H_2O and CO_2, silicate solubility in the fluid results in lowered a_{H_2O}. However, if lack of correspondence between the experimental data and calculations (taking biotite and orthopyroxene solid-solutions as ideal) were due to the effect of a silicate component in the fluid, the a_{H_2O} would have to be about 0.7 (at X_{Ann} = 0.5). With a silicate component of only 7 to 10 wt% in the fluid, this seems an unreasonably large effect. Thus, it appears that phlogopite-annite solid-solution must be significantly non-ideal and/or enstatite-ferrosilite solid-solution must have significantly negative mixing parameters. Ignoring this in any calculations results in any calculated a_{H_2O} being too low.

Natural biotites practically never have compositions that can be represented adequately as micas on the phlogopite-annite join. Excess Al, Ti, F, Cl, and other elements are always present and will shift the positions of the equilibria (e.g., Peterson et al. 1991; Patiño Douce 1993; Dooley and Patiño Douce 1996). The solubility of silicate components in the fluid should also be taken into account. Until the uncertainties surrounding the activity-composition relations in biotite and orthopyroxene solid-solutions are removed, estimation of a_{H_2O} and X_{H_2O} will remain problematical. Moreover, results of attempts to calculate X_{H_2O} or to model equilibria with minerals having compositions outside the experimentally investigated field will be unreliable.

CO_2 and crustal melting

One clear implication of the present results is that the presence of CO_2 in the fluid phase coexisting with an assemblage of Bt+Qtz±Kfs will not have any fluxing effect on partial melting. For practical purposes, at these P-T conditions, CO_2 is an inert fluid component. As in studies on the KMASH system (Clemens 1993; Clemens et al. 1997), CO_2 merely acts to reduce a_{H_2O}, allowing the dehydration reaction to occur at lower T but shifting all melting equilibria toward higher T. Under no circumstances will CO_2 influx cause a lowering of the solidus in crustal, biotite-bearing rocks.

The present work sheds no light on the nature of the low-silica, potassic, highly magnesian, ''glassy'' phase reported in the products of the Peterson and Newton (1989b, 1990) experiments. It has been suggested that this material might be some form of amorphous, fluid-phase quench product. We certainly identified fluid-phase quench material in the products of our experiments. However, the composition of this material (very high SiO_2 and very low MgO+ FeO and K_2O) is completely unlike the ''glasses'' described by Peterson and Newton (Table 3). The origin of the Peterson and Newton ''glassy'' material remains obscure. Its composition suggests that it may have been a mixture of fluid-phase quench and crystals. Whatever this material was, it was not a quenched melt phase.

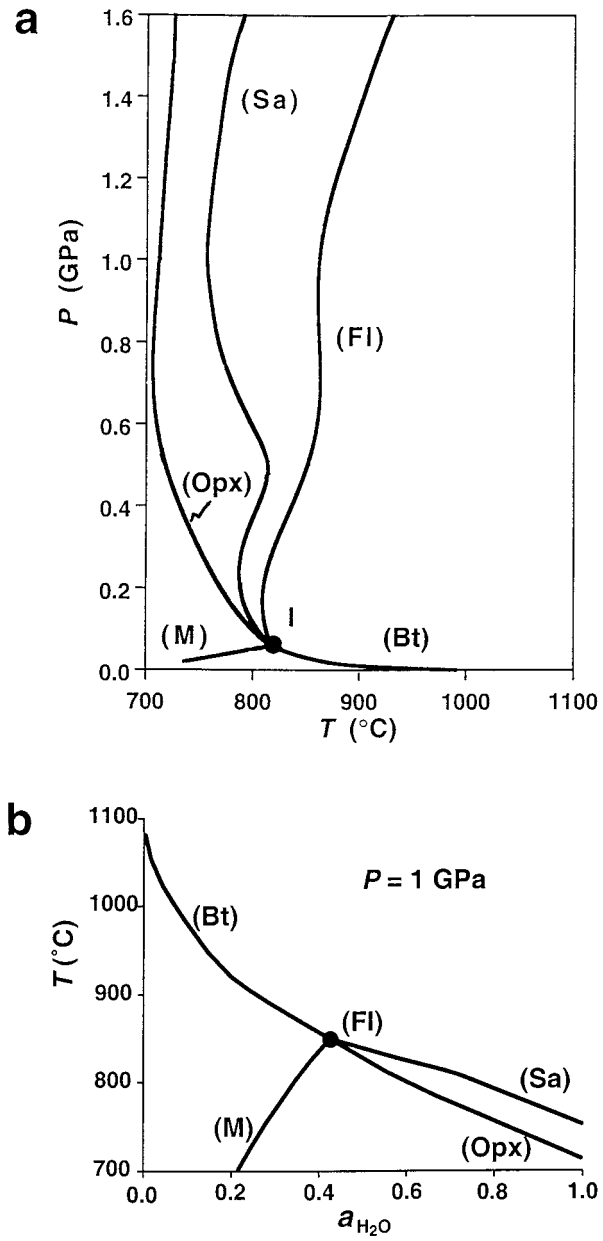

FIGURE 5. (**a**) *P-T* and (**b**) isobaric T-a_{H_2O} sections through the quartz-saturated portion of the system $KAlO_2$-MgO-FeO-SiO_2-H_2O, for $X_{Fe} = 0$, based on the work of Vielzeuf and Clemens (1992), Clemens (1995), and Clemens et al. (1997), showing the univariant equilibria surrounding the invariant point (I), involving the phases Bt, Opx, Sa, Qtz, M, and Fl. The equilibria (labeled according to the absent phase) are:

$$\text{Bt} + \text{Qtz} = \text{Opx} + \text{Sa} + \text{Fl} \quad \text{(M)}$$

$$\text{Bt} + \text{Qtz} + \text{Sa} + \text{Fl} = \text{M} \quad \text{(Opx)}$$

$$\text{Bt} + \text{Qtz} + \text{Fl} = \text{Opx} + \text{M} \quad \text{(Sa)}$$

$$\text{Bt} + \text{Qtz} = \text{Opx} + \text{Sa} + \text{M} \quad \text{(FL)}$$

and

$$\text{Opx} + \text{Qtz} + \text{Sa} + \text{Fl} = \text{M}. \quad \text{(Bt)}$$

These reaction labels are also used in figures 2, 3, 6, and 7. The *P-T* section a can be used to appreciate the locations of equilibria shown in Figures 3, 4, 6b, and 7 and the T-X_{H_2O} section b for the equilibria shown in Figure 6a.
←

Partial melting in fluid-deficient (rock-dominated) systems

Equilibria involving micas are considered critical in the formation and crystallization of migmatites and granitic magmas (see Clemens 1995). It is worth considering the effect of variable biotite composition on the positions of partial melting reactions when the fluid-rock ratio is low and hydration-dehydration reactions control the fluid composition.

In the Fe-free model system KMASH-CO_2, equilibria involve phlogopite, enstatite, sanidine, quartz, melt, and H_2O-CO_2 fluid (Greenwood 1975; Thompson 1990; Clemens 1990, 1993; Vielzeuf and Clemens 1992; Zharikov 1994). Figure 5 shows the equilibria in the Fe- and CO_2-free system, and should be referred to for orientation in the discussion of subsequent figures. Figure 6 shows the locations of some important quartz-present equilibria in the system with CO_2 present as a component. In the polybaric T-X_{H_2O} diagram of Figure 6a, the curve U traces the location of the isobaric invariant point, which shifts toward higher T and lower X_{H_2O} as P increases. Note that this isobaric invariant point corresponds to the only univariant equilibrium in the system (Phl+Qtz+Fl = En+Sa+M, designated reaction U by Clemens et al. 1997).

Now consider a rock containing biotite+quartz±alkali feldspar, and an H_2O-CO_2 fluid phase. Starting with $X_{H_2O} < 1$, as the temperature and pressure increase along path A the reaction Phl+Qtz = En+Sa+H_2O (M) will be initiated at point a (Fig. 6a and 6b). With a tiny amount of intergranular fluid present, dehydration of a very small quantity of biotite would cause an increase in X_{H_2O}. If there were no fluid loss from the system, the increase in X_{H_2O} and pore pressure would halt the dehydration reaction. Since the *P-T* path during metamorphism is externally imposed (by tectonics), reaction could not continue to follow the univariant curve toward I′. The assemblage Sa+En+Fl would not be developed.

As X_{H_2O} increased, conditions appropriate to fluid-present melting might be reached, because the fluid-present melting reaction (M) would shift to a lower temperature. At point b, the univariant melting reaction would be encountered. Here, all H_2O released by biotite breakdown would be dissolved in the melt phase, and would not affect the composition of any equilibrium fluid. The melt proportion formed would be controlled by the bulk composition of the system and the solubility of H_2O in the melt (increasing with P). Melting would continue until either mica or quartz was consumed.

Now consider path B (Figs. 6a and 6b) in which the

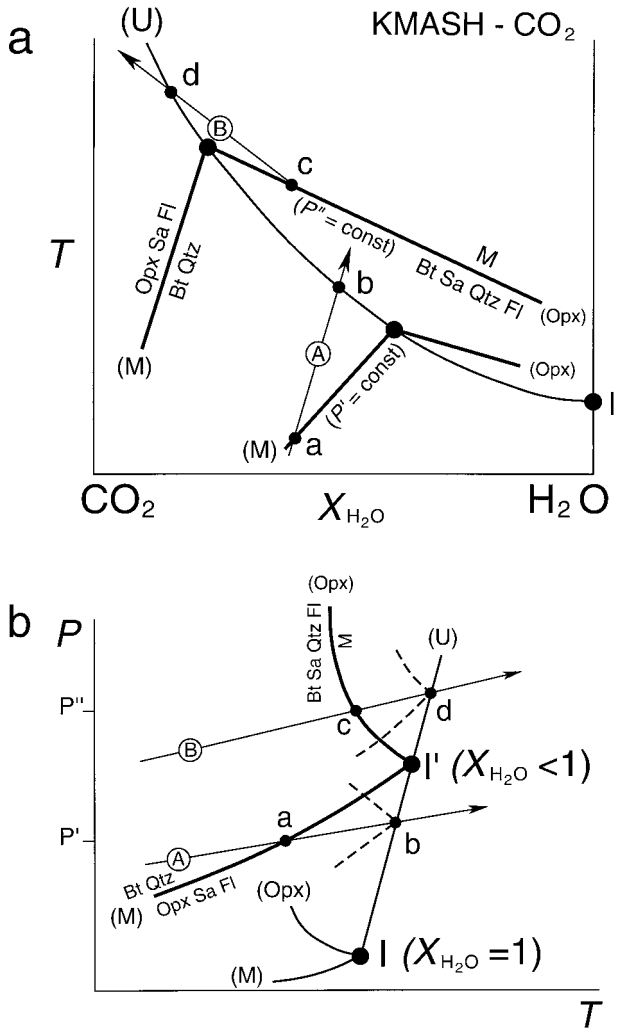

FIGURE 6. Schematic polybaric T-X_{H_2O} (**a**) and P-T (**b**) diagrams showing the positions of some important reactions in the system KMASH-CO_2 with fluid compositions buffered by mineral reactions. Reactions are labeled according to the absent phase (cf., Fig. 2 in Clemens et al. 1997). The curve labeled (U) is the univariant melting reaction, almost coincident with the fluid-absent reaction in the CO_2-free system (Clemens et al. 1997). In the P-T section, note that the invariant point shifts to higher P and T as X_{H_2O} decreases, and toward lower P and T as X_{H_2O} increases, terminating at I when $X_{H_2O} = 1$. See the text for discussion of the evolution of the system (paths A and B, in circles) and the meanings of points a, b, c, and d. I′ is the invariant point in the initial state.

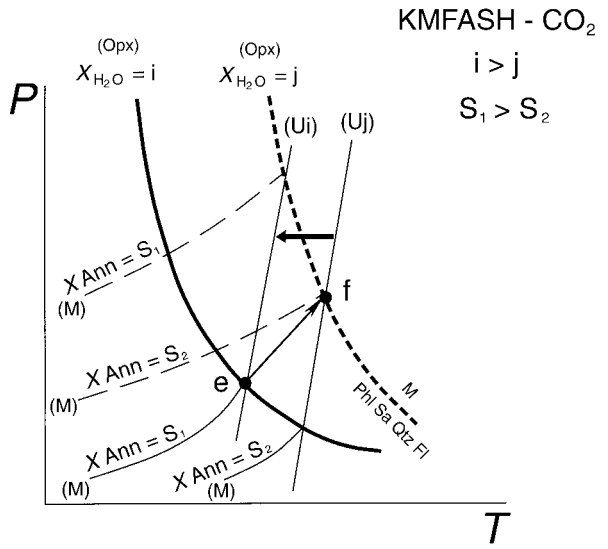

FIGURE 7. Schematic P-T diagram showing the positions of univariant, fluid-present solidus reactions (thick lines) and isopleths of biotite composition (thin lines) in the system KMFASH-CO_2, where fluid composition is buffered by mineral reactions (a rock-dominated, rather than a fluid-dominated system). Solid lines are for equilibria at X_{H_2O} = i, and dashed lines are for X_{H_2O} = j. The broad arrow shows the direction in which the univariant reaction (or the fluid-absent reaction) shifts with increased X_{Fe}. See the text for detailed discussion.

starting X_{H_2O} and P are appropriate to cause congruent melting on reaction (Opx) at point c. Formation of the first drop of melt would result in decreased X_{H_2O}, since CO_2 is far less soluble in the melt than in the fluid, and the quantity of phlogopite dissolved in the melt is miniscule (Clemens and Wall 1981; Vielzeuf and Clemens 1992; Puziewicz and Johannes 1990; Clemens 1995).

The P-T-X_{H_2O} of path B will eventually intersect the incongruent melting reaction (Sa). Here, biotite would start to break down in larger quantities, with the formation of orthopyroxene. The amount of H_2O released by biotite breakdown would be insufficient to compensate for dissolution of H_2O in the melt. The stoichiometry of the melting reaction is such that the melt can always dissolve more H_2O than is contained in the subsolidus Phl+Qtz assemblage. The only exception is possibly at P < 100 MPa (Vielzeuf and Clemens 1992). In any case, the dissolution of H_2O in the melt would result in the fluid becoming enriched in CO_2. As temperature and pressure rose, X_{H_2O} would decrease and the initial mineral assemblage (Bt+Qtz) would be preserved, provided that the system remained at equilibrium. At lower X_{H_2O}, the melting reaction would shift to higher T and P. On attaining point d (analogous to point b on path A), the univariant melting reaction (U) would be encountered, and the subsequent evolution would be similar to that described for path A.

Next consider the system with Fe in addition to Mg, with a starting biotite of $X_{Ann} = S_1$ (Fig. 7). Before any melting, and with dehydration of biotite, the evolution of the system would be similar to that described above. An invariant point (point e in Fig. 7) would exist for a fixed biotite composition. However, isopleths of biotite composition in the subsolidus divariant assemblage shift toward lower T with increased X_{Fe} (Figs. 2 and 3). Hence, melting would take place at lower T with Fe added to the system.

In Figure 7, point e corresponds to initial melting at

X_{H_2O} = i and X_{Ann} = S_1. In nature, orthopyroxene would be more Fe-rich than coexisting biotite. However, we have assumed that the bulk starting composition lies on the biotite-quartz join or in the biotite-quartz-sanidine plane (see Fig. 1). Thus, X_{Ann} remains fixed and equal to X_{Fe} of the bulk system. Considering a *P-T* path such as B in Figure 6, as a consequence of this choice, orthopyroxene could not be formed at point e. Thus, in contrast to the Fe-free system, no melt would be formed here for the biotite composition in question. At a higher starting X_{H_2O}, or with a more Fe-rich biotite, melting *would* occur at e.

Melting reactions involving biotite and orthopyroxene here are continuous in *P-T*-X_{H_2O}-X_{Fe} space. Thus, an increase in *T* and *P*, in the direction e-f (Fig. 7), would cause fluid-present melting and a shift in biotite composition toward lower X_{Fe}. Along path e-f, orthopyroxene with X_{Fe} greater than S_1 and biotite with X_{Fe} less than S_1 would form, while biotite would be progressively consumed. If the amount of fluid in the system were limited (i.e., in a rock-dominated system), processes similar to those occurring along path B (in the Fe-free system; Fig. 6) would occur. If quartz were completely consumed by the melting reaction, or X_{Fe} were to reach the value of S_1 (i.e., biotite completely consumed), the stable assemblage would be Opx+Kfs+Qtz+melt, and X_{H_2O} would decrease to the value of j.

All of the above discussion assumes that the rates of biotite breakdown reactions are sufficiently fast that near-equilibrium conditions are maintained as *P* and/or *T* change with time during metamorphism. Under conditions of disequilibrium there can be some rather interesting effects. For example, Clemens et al. (1997) considered disequilibrium conditions in such a rock-dominated system. They concluded that subsolidus dehydration on (M) could precede local metastable melting on (Sa), and that such behavior could explain some apparent field examples of melting associated with the flow of CO_2-rich fluid along fractures. In the present context it is worth noting that if metamorphic *P* rises faster than biotite dehydration and fluid-absent or univariant fluid-present melting can occur, those reactions will either cease or not occur at all. This limitation on melting occurs because such reactions have positive d*P*/d*T* slopes for any given X_{Fe}. Little is currently known about the rates of these reactions. Although reactions in KMASH are indeed sluggish, the kinetics appear to improve at higher *P* (Vielzeuf and Clemens 1992; Clemens 1995). The persistence of disequilibrium four-phase mineral assemblages in the products of the present experiments demonstrates that the kinetics remain sluggish when Fe is added to the system. Nevertheless, we suggest that the generally very slow rates of tectonic burial would tend to favor the maintenance of equilibrium in natural rocks. There is clearly a need for detailed kinetic studies of biotite dehydration and partial melting reactions.

Considering the experimental data of Vielzeuf and Montel (1994), on melting of metagraywackes under fluid-absent conditions, there must be a divariant temperature interval over which orthopyroxene appears and biotite disappears. The width of this interval ranges from 50 to 90 °C, depending on the pressure. Using the partitioning relationships between biotite and orthopyroxene determined by Fonarev and Konilov (1986), we would expect a divariant interval (in which biotite would coexist with orthopyroxene and melt) of no more than 30 °C. Thus, it seems probable that the formation of phases such as ilmenite and magnetite, as products of melting reactions (see Vielzeuf and Montel 1994, Table 2), would decrease X_{Fe} of biotite, expanding its thermal stability and broadening the divariant interval (see also Stevens et al. 1997).

Acknowledgments

This study was supported by the Russian Foundation for Fundamental Studies (project 95-05-15304a), the Royal Society of Great Britain, INTAS (project INTAS-94-2466), all to A.A.G and A.N.K, and U.K. Natural Environment Research Council Grant GR3/7669 to J.D.C. Linda Parry drafted the final versions of the figures at Kingston. An earlier version of the paper was read by Alberto Patiño and Tracy Rushmer and we thank them for their helpful comments. The penultimate version was reviewed by Jim Grant and Bob Tracy, who we also thank for advice and suggested improvements. The editorial ministrations of Robert Dymek are also much appreciated.

References cited

Aranovich, L.Ya. and Kosyakova, N.A. (1986) Equilibrium cordierite+orthopyroxene+quartz: Experimental data and thermodynamics of ternary Fe-Mg-Al orthopyroxene solid solution. Geokhimiya, 8, 1181–1201 (in Russian).

Aranovich, L.Ya. and Newton, R.C. (1998) Reversed determination of the reaction: phlogopite+quartz = enstatite+potassium feldspar+H_2O in the ranges 750–875 °C and 2–12 kbar at low H_2O activity with concentrated KCl solutions. American Mineralogist, 83, 193–204.

Aranovich, L.Ya. and Podlesskii, K.K. (1989) Geothermobarometry of high-grade metapelites: simultaneously operating reactions. In J.S. Daly, R.A. Cliff, and B.W.D. Yardley, Eds., Evolution of Metamorphic Belts, Geological Society Special Publication 43, p. 45–61.

Berman, R.G., Aranovich, L.Y., Gekin, M., and Mäder, U.K. (1995) Phase equilibrium constraints on the stability of biotite: Part 1. Mg-Al biotite in the system K_2O-MgO-Al_2O_3-SiO_2-H_2O-CO_2. Current Reseach (Geological Survey of Canada), 1995E, 253–261.

Bhattacharya, A., Raith, M., Langen, R., and Sen, S.K. (1992) Non-ideal mixing in the phlogopite-annite binary: Constraints from experimental data on Mg-Fe partitioning and a reformulation of the biotite-garnet geothermometer. Contributions to Mineralogy and Petrology, 111, 87–93.

Bohlen, S.R., Boettcher, A.L., Wall, V.J., and Clemens, J.D. (1983) Stability of phlogopite-quartz and sanidine-quartz: A model for melting in the lower crust. Contributions to Mineralogy and Petrology, 83, 270–277.

Carpenter, M.A. and Salje, E.K.H. (1994) Thermodynamics of nonconvergent cation ordering in minerals. II. Spinels and the orthopyroxene solid solution. American Mineralogist, 79, 1068–1083.

Circone, S. and Navrotsky, A. (1992) Substitution of $^{[6,4]}$Al in phlogopite: High-temperature solution calorimetry, heat capacities, and thermodynamic properties of the phlogopite-eastonite join. American Mineralogist, 77, 1191–1205.

Clemens, J.D. (1981) Origin and evolution of some Peraluminous Acid Magmas, 577 p. Ph.D. thesis, Monash University, Clayton, Victoria, Australia.

——(1990) The granulite-granite connexion. In D. Vielzeuf and Ph. Vidal, Eds., p. 25–36. Granulites and Crustal Evolution, Kluwer Academic Publishers, Dordrecht, the Netherlands.

——(1993) Experimental evidence against CO_2-promoted deep crustal melting. Nature, 363, 336–338.

———(1995) Phlogopite stability in the silica-saturated portion of the system $KAlO_2$-MgO-SiO_2-H_2O: New data and a reappraisal of phase relations to 1.5 GPa. American Mineralogist, 80, 982–997.

Clemens, J.D. and Wall, V.J. (1981) Crystallization and origin of some peraluminous (S-type) granitic magmas. Canadian Mineralogist, 19, 111–132.

Clemens, J.D., Circone, S., Navrotsky, A., McMillan, P.F., Smith, B.K., and Wall, V.J. (1987) Phlogopite: High temperature solution calorimetry, thermodynamic properties, Al-Si and stacking disorder, and phase equilibria. Geochimica et Cosmochimica Acta, 51, 2569–2578.

Clemens, J.D., Droop, G.T.R., and Stevens, G. (1997) High-grade metamorphism, dehydration and crustal melting: A reinvestigation based on new experiments in the silica-saturated portion of the system $KAlO_2$-MgO-SiO_2-H_2O-CO_2 at P = 1.5 GPa. Contributions to Mineralogy and Petrology, 129, 308–325.

Dooley, D.F. and Patiño Douce, A. (1996) Fluid-absent melting of F-rich phlogopite+rutile+quartz. American Mineralogist, 81, 202–212.

Ferry, J.M. and Spear, F.S. (1978) Experimental calibration of the partitioning of Fe and Mg between biotite and garnet. Contributions to Mineralogy and Petrology, 66, 113–117.

Fonarev, V.I. and Konilov, A.N. (1986) Experimental study of Fe-Mg distribution between biotite and orthopyroxene at P = 490 MPa. Contributions to Mineralogy and Petrology, 93, 227–235.

Grant, J.A. (1985) Phase equilibria in partial melting of pelitic rocks. In J.R. Ashworth, Ed., Migmatites, p. 86–144. Blackie & Son, Glasgow, U.K.

Graphchikov, A.A. and Konilov A.N. (1996) Experimental study of partial melting of biotite-orthopyroxene-quartz bearing assemblages in the system $KAlO_2$-MgO-FeO-SiO_2-H_2O. European Journal of Mineralogy, 8, 143–152.

Greenwood, H.J. (1975) The buffering of pure fluids by metamorphic reactions. American Journal of Science, 275, 573–593.

Hansen, E.C., Newton, R.C., and Janardhan, A.S. (1984) Fluid inclusions in rocks from the amphibolite-facies gneiss to charnockite progression in southern Karnataka, India: Direct evidence concerning the fluids of granulite metamorphism. Journal of Metamorphic Geology, 2, 249–264.

Hayob, J.L., Bohlen, S.R., and Essene, E.J. (1993) Experimental investigation and application of the equilibrium rutile+orthopyroxene = quartz+ilmenite. Contributions to Mineralogy and Petrology, 115, 18–35.

Hemingway, B.S. (1987) Quartz: Heat capacities from 340 to 1000 K and revised values for the thermodynamic properties. American Mineralogist, 72, 273–279.

Hoffer, E. and Grant, J.A. (1980) Experimental investigation of the formation of cordierite-orthopyroxene paragenesis in pelitic rocks. Contributions to Mineralogy and Petrology, 73, 15–22.

Holland, T.J.B. and Powell, R. (1990) An enlarged and updated internally consistent thermodynamic dataset with uncertainties and correlations: The system K_2O-Na_2O-CaO-MgO-MnO-FeO-Fe_2O_3-Al_2O_3-TiO_2-SiO_2-C-H_2-O_2. Journal of Metamorphic Geology, 8, 89–124.

Holloway, J.R. (1987) Igneous fluids. In Mineralogical Society of America Reviews in Mineralogy, 17, 211–233.

Kerrick, D.M. and Jacobs, G.K. (1981) A modified Redlich-Kwong equation for H_2O, CO_2 and H_2O-CO_2 mixtures at elevated pressures and temperatures. American Journal of Science, 281, 735–767.

Konilov, A.N. and Fonarev, V.I. (1993) An experimental study of the charnockite assemblage biotite+orthopyroxene+K-feldspar+quartz. Petrology, 1, 224–240.

Mueller, R.F. (1972) Stability of biotite: A discussion. American Mineralogist, 57, 300–316.

Nicholls, J. and Stout, M.Z. (1982) Heat effects of assimilation, crystallization, and vesiculation in magmas. Contributions to Mineralogy and Petrology, 81, 326–339.

Patiño Douce, A.E. (1993) Titanium substitution in biotite: An empirical model with applications to thermometry, O_2 and H_2O barometries, and consequences for biotite stability. Chemical Geology, 108, 133–162.

Patiño Douce, A.E., Johnston, A.D., and Rice, J.M. (1993) Octahedral excess mixing properties in biotite: a working model with applications to geobarometry and geothermometry. American Mineralogist, 78, 113–131.

Perchuk, L.L. and Lavrent'eva, I.V. (1983) Experimental investigation of exchange equilibria in the system cordierite-garnet-biotite. In S.K. Saxena, Ed., Kinetics and Equilibrium in Mineral Reactions, p. 199–239. Springer, New York.

Peterson, J.W. and Newton, R.C. (1989a) Reversed experiments on biotite-quartz-feldspar melting in the system KMASH: Implications for crustal anatexis. Journal of Geology, 97, 465–485.

———(1989b) CO_2-enhanced melting of biotite-bearing rocks at deep-crustal pressure-temperature conditions. Nature, 340, 378–380.

———(1990) Experimental biotite-quartz melting in the KMASH-CO_2 system and the role of CO_2 in the petrogenesis of granites and related rocks. American Mineralogist, 75, 1029–1042.

Peterson, J.W., Chacko, T., and Kuehner, S.M. (1991) The effects of fluorine on the vapor-absent melting of phlogopite+quartz: Implications for deep-crustal processes. American Mineralogist, 76, 470–476.

Puziewicz, J. and Johannes, W. (1990) Experimental study of a biotite-bearing granitic system under water-saturated and water-undersaturated conditions. Contributions to Mineralogy and Petrology, 104, 397–406.

Sack, R.O. and Ghiorso, M.S. (1989) Importance of considerations of mixing properties in establishing an internally consistent thermodynamic database: Thermochemistry of minerals in the system Mg_2SiO_4-Fe_2SiO_4-SiO_2. Contributions to Mineralogy and Petrology, 102, 41–68.

Shaw, H.R. (1963) The four-phase curve sanidine-quartz-liquid-gas between 500 and 4,000 bars. American Mineralogist, 48, 883–896.

Stevens, G., Clemens, J.D., and Droop, G.T.R. (1997) Melt production during granulite-facies anatexis: experimental data from "primitive" metasedimentary protoliths. Contributions to Mineralogy and Petrology, 128, 352–370.

Thompson, A.B. (1990) Heat, fluids, and melting in the granulite facies. In D. Vielzeuf and Ph. Vidal, Eds., Granulites and Crustal Evolution, p. 35–57. Kluwer Academic Publishers, Dordrecht, the Netherlands.

Van der Pluijm, B.A., Lee, J.H., and Peacor, D.R. (1988) Analytical electron microscopy and the problem of potassium diffusion. Clays and Clay Minerals, 36, 498–504.

Vielzeuf, D. and Clemens, J.D. (1992) The fluid-absent melting of phlogopite+quartz: Experiments and models. American Mineralogist, 77, 1206–1222.

Vielzeuf, D. and Montel, J.M. (1994) Partial melting of metagreywackes. Part I. Fluid-absent experiments and phase relationships. Contributions to Mineralogy and Petrology, 117, 375–393.

Vinograd, V.L. (1995) Substitution of $^{[4]}Al$ in layer silicates: Calculation of the Al-Si configurational entropy according to ^{29}Si NMR spectra. Physics and Chemistry of Minerals, 22, 87–98.

Wendlandt, R.F. (1981) Influence of CO_2 on melting of model granulite facies assemblages: A model for the genesis of charnockites. American Mineralogist, 66, 1164–1174.

Wendlandt, R.F. and Eggler, D.H. (1980) The origin of potassic magmas: 2. Stability of phlogopite in natural spinel lherzolite and in the system $KAlSiO_4$-MgO-SiO_2-H_2O-CO_2 at high pressures and high temperatures. American Journal of Science, 280, 421–458.

Wilkinson, J.J., Rankin, A.H., and Nolan, J. (1996) Silicothermal fluid: A novel medium for mass transport in the lithosphere. Geology, 24, 1059–1062.

Wones, D.R. (1963) Physical properties of synthetic biotites on the join phlogopite-annite. American Mineralogist, 48, 1300–1320.

Wones, D.R. and Dodge, F.C.W. (1977) The stability of phlogopite in the presence of quartz and diopside. Thermodynamics in Geology, p. 229–247. D. Reidel, Boston.

Wood, B.J. (1976) The reaction phlogopite+quartz = enstatite+sanidine+H_2O. Progress in Experimental Petrology, 6, 17–19.

Yoder, H.S. Jr. and Kushiro, I. (1969) Melting of a hydrous phase: Phlogopite. American Journal of Science, 267A, 558–582.

Zharikov, V.A. (1994) Fluids in geological processes. In K.I. Shmulovich, B.W.D. Yardley, and G.G. Gonchar, Eds., Fluids in the Crust: Equilibrium and Transport Properties, p. 13–42. Chapman & Hall, London, U.K.

Manuscript received October 7, 1997
Manuscript accepted September 14, 1998
Paper handled by Robert F. Dymek